Defocusing of a converging electromagnetic wave by a plane dielectric interface

Sjoerd H. Wiersma and Taco D. Visser

Department of Physics and Astronomy, Free University, De Boelelaan 1081, 1081 HV Amsterdam, The Netherlands

Received November 28, 1994; revised manuscript revceived July 31, 1995; accepted August 14, 1995

We study how a converging spherical wave gets distorted by a plane dielectric interface. The fields in the second medium are obtained by evaluating the m-theory diffraction integral on the interface. The loss of intensity and the form of the intensity distribution are investigated. Examples are presented for various refractive-index contrasts and depths of focus. In general the intensity gets spread out over a volume that is large compared with the case without refractive-index contrast. It was found that moving the focusing lens a distance d toward the interface does not result in an equal shift of the intensity profile. This latter point has important practical implications. © 1996 Optical Society of America

1. INTRODUCTION

The focusing of a plane electromagnetic wave by a lens has been the subject of several studies.[1–13] In this paper we study the more complex situation of a focused wave incident on a plane interface. That is, a lens in medium 1 produces a converging spherical wave that, after crossing an interface with medium 2, gets distorted (see Fig. 1). Both media are assumed to be linear, homogeneous, isotropic, and nonconducting. It is the aim of this study to describe the influence of the interface on the intensity and on the form of the diffraction pattern. The intensity is found to be no longer localized in a small region, as is the case when there is just one medium, but rather is spread out over a larger volume. Our results have implications, for example, for microscopy with immersion-fluid objectives where the interface separates the immersion-oil/cover-glass region from the (usually watery) object. As will be discussed, the difference in refractive indices results in a severe loss of resolution. A highly relevant issue is how the diffraction pattern changes when the focusing lens is moved with respect to the interface. In general, the intensity profile is shifted over a distance that differs a constant factor from that over which the lens is moved.

A closely related problem has been studied by Ling and Lee.[14,15] Whereas we consider a converging spherical wave in medium 1 that gets distorted in medium 2, they calculated which (nonspherical) form the wave front in the first medium must have to produce a perfectly spherical wave in the second medium. Their study has applications in the field of hyperthermia treatment, in which a maximum intensity (and hence a spherical wave) is desired in medium 2. Unlike us, Ling and Lee limited themselves to lossless media (i.e., with electric permittivities ϵ_1 and ϵ_2 that are both real).

Another study of interest[16] uses a scalar theory in the paraxial approximation to calculate the waist shift of a Gaussian beam caused by a dielectric interface.

Also worth mentioning is a paper by Gasper *et al.*[17] in which asymptotic approximations for the transmitted and reflected fields are given.

Our approach is as follows. An incoming plane wave, propagating perpendicular to the interface, is converted by a perfect lens obeying the sine condition[18] into a converging spherical wave (see Fig. 1). In the exit pupil the electromagnetic field on the emerging wave front S_1 is determined. As will be justified, the effects of refraction on the polarization are neglected. Neither the form of the wave front nor the directions of the (time-independent parts of the) electromagnetic vectors are assumed to change while traveling to the interface (ray approximation). This too will be justified. Since the wave converges toward the interface, its amplitude will have increased by an amount determined by the distance traveled, which depends on the polar angle θ. Additionally, a phase factor that is also θ dependent is introduced. Having determined the incident fields on the interface, we derive the transmitted field with the help of Fresnel coefficients. The so-called m theory of diffraction can then be used to calculate the energy density in the region of focus in the second medium. No paraxial approximation is necessary for the developed formalism. The m theory is due to several authors, namely, Smythe,[9] Severin,[10] and Toraldo di Francia.[11] The latter treatment is probably the clearest.

Throughout this paper we use SI units.

2. FIELD ON THE INTERFACE

Consider an incident monochromatic plane wave propagating in the negative z direction that is linearly polarized,

$$\mathbf{E} = \mathbf{E}_{\text{inc}} \exp[i(k_1 \hat{k} \cdot \mathbf{r} + \omega t)], \qquad (z > f) \tag{1}$$

with k_1 the wave number in medium 1 and the electric field amplitude vector

$$\mathbf{E}_{\text{inc}} = (\cos \alpha, \sin \alpha, 0), \tag{2}$$

0740-3232/96/020320-06$06.00

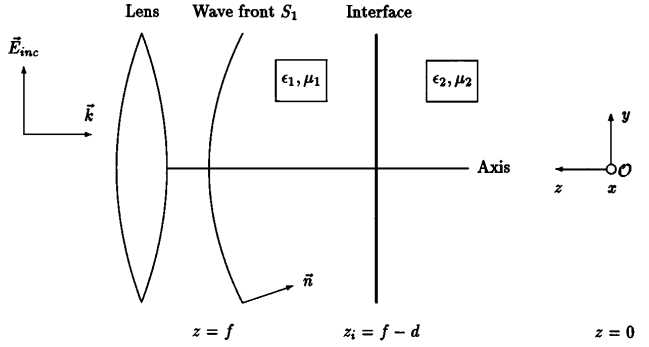

Fig. 1. Definition of the coordinate system. Shown at left are the unit wave vector $\hat{k}$ and the electric vector $\mathbf{E}_{\text{inc}}$, both before refraction by an objective with semiaperture angle Ω. The incoming wave propagates perpendicular to the interface in the $-z$ direction. The origin is placed at a distance f from the exit pupil. $\hat{n}$ is the unit wave vector after refraction by the lens.

where α is the angle of polarization. From here on, we will take $\alpha = 0$ and suppress the harmonic time dependence.

It is assumed that the lens obeys the sine condition,[18] i.e., rays traveling parallel to the z axis emerge at the same lateral distance from the axis as they entered it.

The meridional plane is spanned by the incident unit wave vector $\hat{k}$ and the unit wave vector after refraction $\hat{n}$, with

$$\hat{k} = \begin{pmatrix} 0 \\ 0 \\ -1 \end{pmatrix}, \qquad \hat{n} = -\begin{pmatrix} \sin\theta\cos\phi \\ \sin\theta\sin\phi \\ \cos\theta \end{pmatrix}. \tag{3}$$

The effect of refraction on the polarization angle will be neglected. From the Fresnel equations it follows that this is justified as long as the incoming wave vector does not make an appreciable angle with the normal of the refracting surfaces that make up the lens system. For practical objectives, this seems to be a reasonable assumption. Now the field $\mathbf{E}_{S_1}$ in the exit pupil can be written as the sum of an unchanged component ($\mathbf{E}_s$) of $\mathbf{E}_{\text{inc}}$ that is perpendicular to the meridional plane and a rotated component ($\mathbf{E}_p$) that lies in the meridional plane.[2,13] The first component lies in the direction of $\hat{k} \times \hat{n}$. The second component is normal to both $\hat{k}$ and $\hat{k} \times \hat{n}$, and to points after refraction in the direction of $\hat{n} \times (\hat{k} \times \hat{n})$. Hence

$$\mathbf{E}_s = \frac{\mathbf{E}_{\text{inc}} \cdot (\hat{k} \times \hat{n})}{|\hat{k} \times \hat{n}|^2} (\hat{k} \times \hat{n}), \tag{4}$$

$$\mathbf{E}_p = \frac{\mathbf{E}_{\text{inc}} \cdot [\hat{k} \times (\hat{k} \times \hat{n})]}{|\hat{k} \times (\hat{k} \times \hat{n})||\hat{n} \times (\hat{k} \times \hat{n})|} [\hat{n} \times (\hat{k} \times \hat{n})]. \tag{5}$$

The now normalized directions of decomposition are given by

$$\frac{\hat{k} \times \hat{n}}{|\hat{k} \times \hat{n}|} = \begin{pmatrix} -\sin\phi \\ \cos\phi \\ 0 \end{pmatrix}, \tag{6}$$

$$\frac{\hat{n} \times (\hat{k} \times \hat{n})}{|\hat{n} \times (\hat{k} \times \hat{n})|} = \begin{pmatrix} \cos\theta\cos\phi \\ \cos\theta\sin\phi \\ -\sin\theta \end{pmatrix}, \tag{7}$$

$$\frac{\hat{k} \times (\hat{k} \times \hat{n})}{|\hat{k} \times (\hat{k} \times \hat{n})|} = \begin{pmatrix} \cos\phi \\ \sin\phi \\ 0 \end{pmatrix}. \tag{8}$$

Indulging in a little algebra, we find for the components $\mathbf{E}_s$ and $\mathbf{E}_p$

$$\mathbf{E}_s = \cos^{1/2}\theta \sin\phi \begin{pmatrix} \sin\phi \\ -\cos\phi \\ 0 \end{pmatrix}, \tag{9}$$

$$\mathbf{E}_p = \cos^{1/2}\theta \cos\phi \begin{pmatrix} \cos\theta\cos\phi \\ \cos\theta\sin\phi \\ -\sin\theta \end{pmatrix}. \tag{10}$$

Both components have been multiplied by a factor $\cos^{1/2}\theta$ to account for the aplanatic energy projection by the lens.[15] (Note that E_s has no z component, as is expected.) So the field in the exit pupil S_1 is given by

$$\mathbf{E} = \mathbf{E}_{S_1} \exp[ik_1 \hat{n} \cdot \mathbf{r}], \qquad \text{(in exit pupil)} \tag{11}$$

where

$$\mathbf{E}_{S_1} = \mathbf{E}_s + \mathbf{E}_p. \tag{12}$$

The reader may be assured that indeed $\nabla \cdot \mathbf{E} = 0$, since $\hat{n} \cdot \mathbf{E}_{S_1} = 0$.

Next consider how the field through the spherical segment on S_1 between the angles θ and $\theta + \mathrm{d}\theta$ is changed upon reaching the corresponding ring at the interface. Two factors have to be considered, namely, a phase factor and an amplitude factor, both angle dependent, which we are now about to determine.

The path length for a ray traveling at an angle θ from S_1 to the interface equals $f - t(\theta)$, with

$$t(\theta) = (f - d)/\cos\theta, \tag{13}$$

where f is the focal length of the lens and d is the distance from the exit pupil to the interface (see Fig. 1). So the phase factor $F(\theta)$ that is introduced is

$$F(\theta) = \exp\left[ik_1 \left(f - \frac{f - d}{\cos\theta} \right) \right]. \tag{14}$$

k_i is the wave number in medium i, for which

$$k_i \equiv (\omega^2 \epsilon_i \mu_i)^{1/2}, \qquad (i = 1, 2) \tag{15}$$

where ω denotes the angular frequency and the square root is taken such that $\mathrm{Im}(k_i) \leq 0$.

The area of the spherical segment on S_1 is proportional to f^2, whereas the area of the corresponding ring on the interface is proportional to $t^2(\theta)/\cos\theta$. Conservation of energy requires that the amplitude of the electric field is inversely proportional to the root of the ratio of the respective areas. Hence the amplitude factor $K(\theta)$ that is introduced reads

$$K(\theta) = \frac{f \cos^{3/2}\theta}{f - d}. \tag{16}$$

So we get for the electric field $\mathbf{E}$ incident on the left-hand side of the interface at $z_i = f - d$

$$\mathbf{E}_{\delta|0}(\theta, \phi, z_i + \delta) = K(\theta) F(\theta) \mathbf{E}_{S_1}(\theta, \phi). \tag{17}$$

It should be noted that the use of a vectorial diffraction theory instead of a geometrical approach to calculate the field on the interface would have yielded the very same result. Such a theory, as is due to Wolf [Eq. (3.3) of Ref. 1] and Richards and Wolf [Eq. (2.17) of Ref. 2], describes the focused field as a superposition of plane waves. These waves travel in the direction of the focus (i.e., the origin $\mathcal{O}$ in Fig. 1) and have an amplitude $E_S(\theta)$ given by Eq. (12). Consequently, application of this theory also leads to Eq. (17).

At the right-hand side of the interface, in medium 2, the amplitudes of the electric field components are multiplied by η_s and η_p, the Fresnel coefficients for transmission of the s and p components, respectively. These coefficients depend on the angle of incidence θ and the refractive indices on either side of the interface. The index of refraction n_i is given by $n_i = c\sqrt{\epsilon_i \mu_i}\,(i = 1, 2)$, with c the speed of light *in vacuo*. Whereas the s component of the field remains otherwise unaffected, the component parallel to the plane of incidence ($\mathbf{E}_p$) is also rotated. To find its new form consider the (normalized) direction of propagation $\hat{q}$ of the refracted wave. It is obviously given by

$$\hat{q} = -\begin{pmatrix} \sin\theta' \cos\phi \\ \sin\theta' \sin\phi \\ \cos\theta' \end{pmatrix}, \tag{18}$$

with θ' given by Snell's law as $\theta' = \sin^{-1}[(n_1 \sin\theta)/n_2]$. After refraction, $\mathbf{E}_p$ is perpendicular to both $\hat{q}$ and $\hat{q} \times \hat{n}$; i.e., it is then directed along $\hat{q} \times (\hat{q} \times \hat{n})$. Hence

$$\mathbf{E}_{p;\delta\rfloor 0}(z_i - \delta) = \eta_p |\mathbf{E}_{p;\delta\rfloor 0}(z_i + \delta)| \frac{\hat{q} \times (\hat{q} \times \hat{n})}{|\hat{q} \times (\hat{q} \times \hat{n})|}. \tag{19}$$

Also,

$$\mathbf{E}_{s;\delta\rfloor 0}(z_i - \delta) = \eta_s \mathbf{E}_{s;\delta\rfloor 0}(z_i + \delta), \tag{20}$$

where the (θ, ϕ) dependence is temporarily suppressed. So we find for the total electric field on the right-hand side of the interface

$$\begin{aligned} \mathbf{E}_{\delta\rfloor 0}(z_i - \delta) &= \mathbf{E}_{s;\delta\rfloor 0}(z_i - \delta) + \mathbf{E}_{p;\delta\rfloor 0}(z_i - \delta), \\ &= K(\theta)F(\theta)\cos^{1/2}\theta \left[\eta_s \sin\phi \begin{pmatrix} \sin\phi \\ -\cos\phi \\ 0 \end{pmatrix} \right. \\ &\quad \left. + \eta_p \cos\phi \begin{pmatrix} \cos\theta' \cos\phi \\ \cos\theta' \sin\phi \\ -\sin\theta' \end{pmatrix} \right], \end{aligned} \tag{21}$$

where we have used Eqs. (9), (10), and (19). This is the final expression for the electric field after it has just traversed the interface.

In the formalism that we use, the factor $\hat{m} \times \mathbf{E}$ fully determines the electric field at any point in medium 2.[20] The normal $\hat{m}$ to interface equals (0, 0, 1) (see Fig. 1). So

$$\hat{m} \times \mathbf{E}(\theta, \phi, z_i) = K(\theta)F(\theta)\cos^{1/2}\theta \left[\eta_s \sin\phi \begin{pmatrix} \cos\phi \\ \sin\phi \\ 0 \end{pmatrix} \right.$$
$$\left. + \eta_p \cos\phi \begin{pmatrix} -\cos\theta' \sin\phi \\ \cos\theta' \cos\phi \\ 0 \end{pmatrix} \right]. \tag{22}$$

We have now arrived at our first goal. The relevant field quantity immediately to the right of the interface has been determined. The diffraction integral can now be applied to produce an expression for the field near its new focal region in medium 2.

3. DIFFRACTION INTEGRAL

The so-called m-theory integral[9–11] is used to calculate the diffracted field in medium 2. The solutions satisfy the Maxwell equations. The diffraction integral expresses the diffracted electric field $\mathbf{E}(\mathbf{x})$ in terms of an integral over a plane of a function of the tangential component of $\mathbf{E}$. In a medium with material parameters ϵ_2 and μ_2, the integral reads

$$\mathbf{E}(\mathbf{x}) = 2 \int_S (\hat{m} \times \mathbf{E}) \times \nabla G \, \mathrm{d}\sigma. \tag{23}$$

For S we take the illuminated (circular) region of the interface, which means that we use Eq. (22) for $\hat{m} \times \mathbf{E}$. The Green function G is defined as

$$G(\mathbf{p}, \mathbf{x}) = \frac{\exp(ik_2|\mathbf{x} - \mathbf{p}|)}{4\pi|\mathbf{x} - \mathbf{p}|}, \tag{24}$$

from which

$$\nabla G = \left(\frac{1}{|\mathbf{x} - \mathbf{p}|} - ik_2 \right) G \hat{e}_G. \tag{25}$$

The unit vector $\hat{e}_G$ is directed from a point $\mathbf{p}$ on S, where the integrand is evaluated, to a point $\mathbf{x}$ where the field is calculated:

$$\hat{e}_G = \frac{\mathbf{x} - \mathbf{p}}{|\mathbf{x} - \mathbf{p}|}. \tag{26}$$

The infinitesimal surface element $\mathrm{d}\sigma$ equals the surface element of a sphere with radius $t(\theta)$ projected from the lens onto the interface [see Eq. (13)]:

$$\mathrm{d}\sigma = t^2(\theta)\tan\theta \, \mathrm{d}\theta \mathrm{d}\phi \qquad (0 \le \theta \le \Omega), \tag{27}$$

with Ω the semiaperture angle of the lens. An equation similar to Eq. (23) for the diffracted field $\mathbf{H}$ can also be derived.[10,11] However, since we are interested in the intensity (which is proportional to $|\mathbf{E}|^2$), we do not need that expression here. Notice that it is also possible to express the diffracted fields in terms of the tangential component of $\mathbf{H}$ rather than the tangential component of $\mathbf{E}$.[10]

For the moment we restrict ourselves to the case in which the observation point $\mathbf{x}$ lies on the optical or z axis. There the intensity distribution is independent of the polarization angle α (because of rotational symmetry). We then have for $\hat{e}_G$

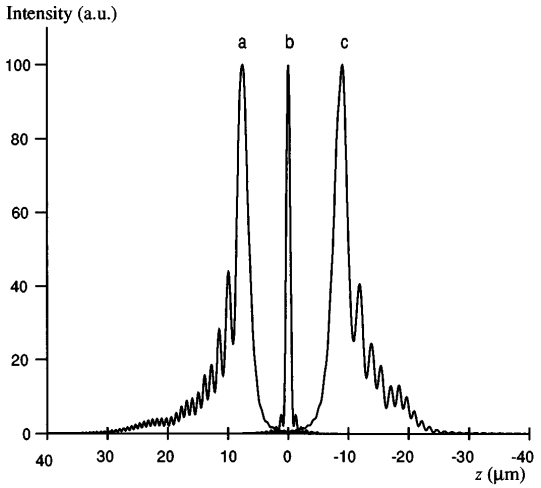

Fig. 2. Axial intensity distribution (in arbitrary units) for $n_1 = 1.51$ and $n_2 = 1.33$ (curve a). At center is shown the intensity profile without contrast, i.e., $n_1 = n_2 = 1.51$ (curve b). Curve c depicts the intensity for $n_1 = 1.33$ and $n_2 = 1.51$. (For all curves $\Omega = 60°$, $\mu_1 = \mu_2 = \mu_0$, $f = 10^{-2}$ m, $f - d = 50$ μm, and $\lambda = 632.8$ nm.) As in all following examples both media are lossless.

$$\hat{e}_G = -\frac{f-d}{s(\theta, z)} \begin{pmatrix} \tan\theta\cos\phi \\ \tan\theta\sin\phi \\ 1 - z/(f-d) \end{pmatrix}, \tag{28}$$

with $|\mathbf{x} - \mathbf{p}|$ abbreviated as $s(\theta, z)$:

$$s(\theta, z) = [t^2(\theta) + z^2 - 2z(f-d)]^{1/2}, \tag{29}$$

where we have used Eq. (13). Computation of the integral as in Eq. (23) yields (using $\omega^2 = k_i^2/\epsilon_i\mu_i$ and $k_0 = 2\pi/\lambda_0$, with λ_0 the free-space wavelength) that the ϕ dependence of the y and z components of the field is such that they vanish on integration. So after integration with respect to ϕ the total electric field on the axis is given by its x component, viz.

$$E_x(0, 0, z) = C \int_0^{\Omega} \exp[i(k_2 s - k_1 t)] g(\theta, z) \mathrm{d}\theta\,, \tag{30}$$

with

$$C(z) = \frac{f}{2}(f-d)^2 \left(\frac{z}{f-d} - 1\right) \exp[ik_1 f]\,, \tag{31}$$

$$g(\theta, z) = \left(\frac{1}{s^3} - \frac{ik_2}{s^2}\right)(\eta_s + \eta_p \cos\theta')\tan\theta\,. \tag{32}$$

When the point of observation $\mathbf{x}$ is not on the axis of symmetry, the function $s(\theta, z)$ gets an additional ϕ dependence, and hence both G and ∇G in Eq. (23) change. Reduction to a one-dimensional integral as just demonstrated is then no longer possible.

4. RESULTS

First, a refractive index mismatch gives rise to an aberrationlike diffraction pattern. An example is presented in Fig. 2. Compared with the intensity distribution without refractive-index contrast (curve b), we see that the interface induces a dramatic asymmetry and broadening of the intensity profile. A long tail with many relatively high secondary maxima extends in the direction of the interface (curve a). The intensity peak is shifted in the same direction.

Using geometrical reasoning it can be shown that the light can reach only a part of the optical axis behind the interface. Let h be the distance from the interface at which a ray with an angle of incidence θ_1 crosses the z axis. We then have

$$h(\theta_1) = (f-d)\frac{\tan\theta_1}{\tan\theta_2} = (f-d)\frac{n_2}{n_1}\frac{\cos\theta_2}{\cos\theta_1}\,. \tag{33}$$

Here θ_2 is the angle of propagation after refraction. The index of refraction n_i for lossless media is given by $n_i = c(\epsilon_i\mu_i)^{1/2}$ with $i = 1, 2$ and c being the speed of light *in vacuo*. So only the part of the axis between $h(0)$ and $h(\Omega)$ is illuminated. For the parameters used for curve a of Fig. 2 we find that the geometrical shadow boundaries

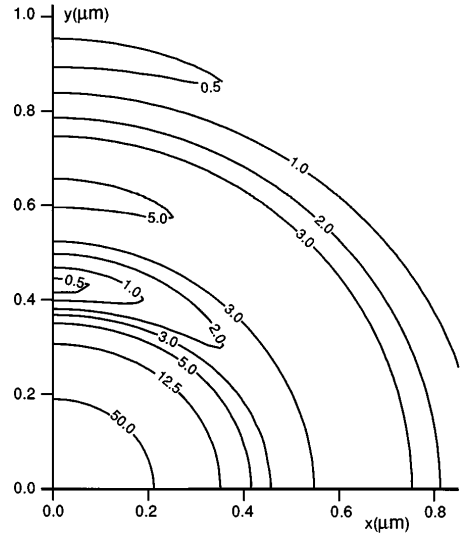

Fig. 3. Isointensity lines (a.u.) in the xy plane of maximum intensity ($z = 7.54$ nm). ($\Omega = 60°$, $\mu_1 = \mu_2 = \mu_0$, $f = 10^{-2}$ m, $f - d = 50$ μm, and $\lambda = 632.8$ nm.)

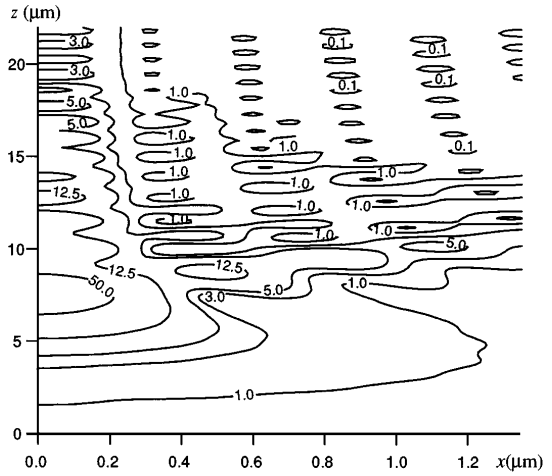

Fig. 4. Isointensity lines (a.u.) in the xz plane ($y = 0$). ($\Omega = 60°$, $\mu_1 = \mu_2 = \mu_0$, $f = 10^{-2}$ m, $f - d = 50$ μm, and $\lambda = 632.8$ nm.) Note: the scale of the two axes is different.

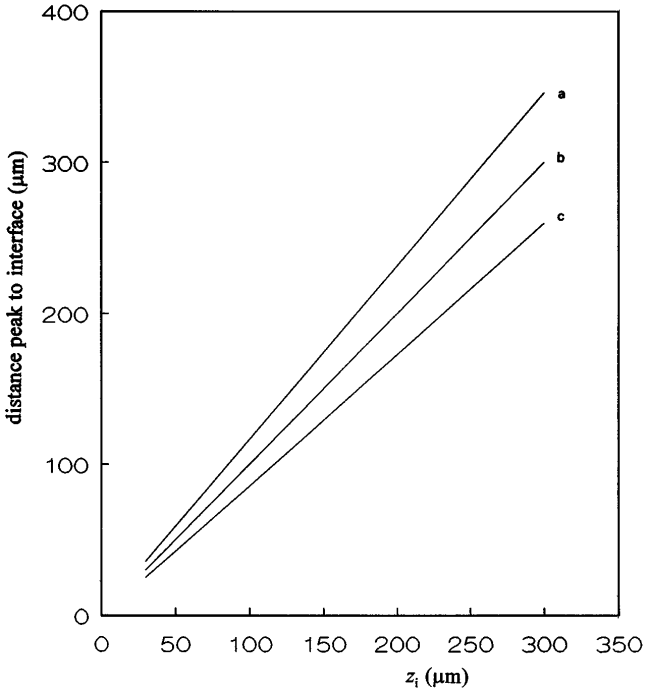

Fig. 5. Distance between the peak and the interface plotted versus the position of the lens. (Note: the distance between the lens and the interface is given by $d = f - z_i$.) Only if $n_1 = n_2$ (curve b) does the peak precisely follow the movement of the lens. If $n_1 > n_2$ (curve c) the peak position shifts less than that of the lens. For $n_1 < n_2$ (curve a) the opposite holds. In all cases $\Omega = 60°$, $\mu_1 = \mu_2 = \mu_0$, $f = 10^{-2}$ m, and $\lambda = 632.8$ nm. In curve a $n_1 = 1.33$, $n_2 = 1.51$, in curve b $n_1 = n_2 = 1.33$, and in curve c $n_1 = 1.51$, $n_2 = 1.33$.

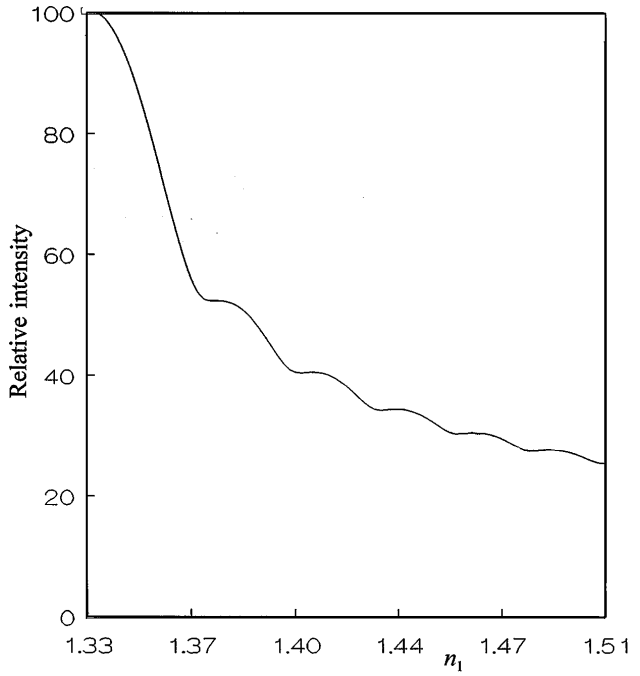

Fig. 6. Peak intensity (a.u.) versus n_1. The index of refraction n_2 is fixed at 1.33. ($\Omega = 60°$, $\mu_1 = \mu_2 = \mu_0$, $f = 10^{-2}$ m, $f - d = 50$ μm, and $\lambda = 632.8$ nm.)

are at $z = 6.0$ μm and $z = 21.8$ μm. We find that the intensity profile indeed falls within this range.

Whereas for curve a of Fig. 2 $n_1 > n_2$, curve c represents the intensity profile for the reverse case, namely, $n_1 < n_2$. We find that the global appearance of the distribution is mirror imaged with respect to the $z = 0$ plane. In this case the geometrical shadow boundaries are at $z = -6.8$ μm and $z = -23.5$ μm. Again we find good agreement. All three curves have been normalized to 100 (see also Fig. 6 below).

In Figs. 3 and 4 the isointensity lines (isophotes) in the xy and xz planes, respectively, are shown for the same parameters. In Fig. 3 polarization is along the horizontal axis. Note that the intensity profile along that axis is substantially broader than that along the other axis.

In Fig. 4 polarization is along the x axis. In this plane the intensity peak is narrower in the x direction than in the z direction. Also, a large number of minima is seen. Figures 3 and 4 clearly differ in appearance from their respective counterparts without refractive-index contrast.[7]

If we move the lens closer to the interface, how much deeper will the point of maximum intensity then lie? This question is answered in Fig. 5. For $n_1 = n_2$ (curve b) the intensity peak follows the movement of the lens precisely. For $n_1 > n_2$ (curve c), however, the peak shift lags behind. For the case that $n_1 < n_2$ (curve a), the peak moves further than the lens does. From Eq. (33) it follows that the paraxial geometrical prediction of the slope equals

$$\frac{\Delta_{\text{peak}}}{\Delta_{\text{lens}}} = -\frac{\partial h(\theta = 0)}{\partial d} = \frac{n_2}{n_1}. \tag{34}$$

As it turns out, this is an acceptable approximation for this range of n_i, even though Ω is large (i.e., nonparaxial).

This effect has great consequences for (confocal) three-dimensional microscopy, in which one commonly uses oil-immersion objectives ($n_1 = 1.51$) to study watery objects ($n_2 = 1.33$). The shift of the object stage is frequently mistaken for the shift in the point that is imaged. As demonstrated in Ref. 21, objects may appear much larger (in the z direction) than they actually are when this effect is not taken into account.

In Fig. 6 the peak intensity is shown for increasing refractive contrast. That is, n_2 is kept at 1.33 while n_1 varies between 1.33 and 1.51. With increasing n_1 the intensity drops dramatically. This is due to two factors: (1) increasing phase differences between waves emanating from different points on the interface and (2) a decrease in transmission through the interface.

In our examples we have used parameters in the range of practical optics. However, the developed formalism is generally applicable.

5. CONCLUSIONS

We have studied the effects of a plane interface on an incident focused electromagnetic wave. The interface causes a strong broadening of the intensity distribution compared with the case where there is no interface. Also, the intensity profile becomes highly asymmetrical.

We found that an increase in the difference in refractive indices $n_1 - n_2$ leads to a dramatic drop in intensity.

Moving the lens over a distance Δ_{lens} with respect to the interface causes a shift in the position of the peak intensity called Δ_{peak}. A result with important applications (e.g., for microscopy) is that the intensity peak does

not precisely follow the movement of the lens. Instead we found that $\Delta_{\text{peak}}/\Delta_{\text{lens}} \sim n_2/n_1$. In practice, this factor can differ significantly from 1.

ACKNOWLEDGMENT

The authors thank A. T. de Hoop for critical comments.

Correspondence should be addressed to T. D. Visser at the address on the title page.

REFERENCES

1. E. Wolf, "Electromagnetic diffraction in optical systems. I. An integral representation of the image field," Proc. R. Soc. London A **253,** 349–357 (1959).
2. B. Richards and E. Wolf, "Electromagnetic diffraction in optical systems, II. Structure of the image field in an aplanatic system," Proc. R. Soc. London A **253,** 358–379 (1959).
3. F. Kottler, *Progress in Optics,* E. Wolf, ed. (North-Holland, Amsterdam, 1965), Vol. IV, pp. 283–314.
4. F. Kottler, *Progress in Optics,* E. Wolf, ed. (North-Holland, Amsterdam, 1967), Vol. VI, pp. 333–377.
5. B. Karczewski and E. Wolf, "Comparison of three theories of electromagnetic diffraction at an aperture. Part I: coherence matrices," J. Opt. Soc. Am. **56,** 1207–1214 (1966).
6. B. Karczewski and E. Wolf, "Comparison of three theories of electromagnetic diffraction at an aperture. Part II: the far field," J. Opt. Soc. Am. **56,** 1214–1219 (1966).
7. A. Boivin and E. Wolf, "Electromagnetic field in the neighborhood of the focus of a coherent beam," Phys. Rev. **138,** B1561–B1565 (1965).
8. C. J. Bouwkamp, "Diffraction theory," Rep. Prog. Phys. **17,** 35–100 (1954).
9. W. R. Smythe, "The double current sheet in diffraction," Phys. Rev. **72,** 1066–1070 (1947).
10. H. Severin, "Zur Theorie der Beugung elektromagnetischer Wellen," Z. Phys. **129,** 426–439 (1951).
11. G. Toraldo di Francia, *Electromagnetic Waves* (Interscience, New York, 1955).
12. B. B. Baker and E. T. Copson, *The Mathematical Theory of Huygen's Principle,* 2nd ed. (Clarendon, Oxford, 1950).
13. T. D. Visser and S. H. Wiersma, "Diffraction of converging electromagnetic waves," J. Opt. Soc. Am. A **9,** 2034–2047 (1992).
14. H. Ling and S-W. Lee, "Focusing of electromagnetic waves through a dielectric interface," J. Opt. Soc. Am. A **1,** 965–973 (1984).
15. J. J. Stamnes, *Waves in Focal Regions* (Hilger, Bristol, UK, 1986). This reference gives an alternative account of the work of Ling and Lee.
16. S. Nemoto, "Waist shift of a Gaussian beam by plane dielectric interfaces," Appl. Opt. **27,** 1833–1839 (1988).
17. J. Gasper, G. C. Sherman, and J. J. Stamnes, "Reflection and refraction of an arbitrary electromagnetic wave at a plane interface," J. Opt. Soc. Am. **66,** 955–961 (1976).
18. M. Born and E. Wolf, *Principles of Optics,* 6th ed. (Pergamon, Oxford, 1980).
19. J. A. Stratton and L. J. Chu, "Diffraction theory of electromagnetic waves," Phys. Rev. **56,** 99–107 (1939).
20. J. A. Stratton, *Electromagnetic Theory* (McGraw-Hill, New York, 1941). This book gives a clear derivation of the uniqueness theorem.
21. T. D. Visser and J. L. Oud, "Volume measurements in 3-D microscopy," Scanning **16,** 198–200 (1994).